Hydrological Sciences Journal

ISSN: 0262-6667 (Print) 2150-3435 (Online) Journal homepage: www.tandfonline.com/journals/thsj20

Impact of land use and land cover changes on water balance in the Ouémé River basin, West Africa

Ernestina Annan, Fabian Merk, William Amponsah, Kwaku Amaning Adjei, Markus Disse & Wilson Agyei Agyare

To cite this article: Ernestina Annan, Fabian Merk, William Amponsah, Kwaku Amaning Adjei, Markus Disse & Wilson Agyei Agyare (21 Jul 2025): Impact of land use and land cover changes on water balance in the Ouémé River basin, West Africa, Hydrological Sciences Journal, DOI: 10.1080/02626667.2025.2516831

To link to this article: https://doi.org/10.1080/02626667.2025.2516831

HYDROLOGICAL SCIENCES JOURNAL
https://doi.org/10.1080/02626667.2025.2516831

SPECIAL ISSUE: TWENTY-FIRST CENTURY HYDROLOGICAL CHALLENGES AND OPPORTUNITIES IN AFRICA

Impact of land use and land cover changes on water balance in the Ouémé River basin, West Africa

Ernestina Annan[a], Fabian Merk[b], William Amponsah[c], Kwaku Amaning Adjei[d], Markus Disse[b] and Wilson Agyei Agyare[c]

[a]WASCAL Climate Change and Land Use, College of Engineering, KNUST, Kumasi, Ghana; [b]Chair of Hydrology and River Basin Management, Technische Universität München (TUM), Munich, Germany; [c]Department of Agricultural and Biosystems Engineering, College of Engineering, KNUST, Kumasi, Ghana; [d]Department of Civil Engineering, College of Engineering, KNUST, Kumasi, Ghana

ABSTRACT

The influence of land use and land cover (LULC) changes on hydrological processes in data-scarce regions such as the Ouémé River basin is unclear, but it is crucial for sustainable water management and flood mitigation. This study assessed the relationship between LULC changes and changes in water balance using four LULC maps and climate data across three periods within 1998–2016 in the Soil and Water Assessment Tool (SWAT). Model calibration yielded NSE $\geq$ 0.8 2, RSR $\leq$ 0.42 and PBIAS ≤ -12.8, while validation yielded NSE $\geq$ 0.81, RSR $\leq$ 0.43 and PBIAS ≤ -14.4. At the basin scale, expansions in agricultural land and settlements/bare land and loss of savanna and forest areas increased runoff by 66% and reduced baseflow (13%), lateral flow (6%), aquifer recharge (7%) and evapotranspiration (1%). Surface runoff was consistently predicted across periods, making it a key water balance indicator. The findings underscore the need for reforestation, sustainable farming and urban planning to mitigate floods.

ARTICLE HISTORY
Received 15 November 2024
Accepted 28 May 2025

EDITOR
S. Archfield

GUEST EDITOR
J-M. Kileshye-Onema

KEYWORDS
Land use and land cover change; hydrological changes; regression; watershed management; West African basin

1 Introduction

Land use and land cover (LULC) have great influence on the hydrological cycle processes, especially in tropical river basins such as the Ouémé River basin, where the linkages between land surface dynamics and water balance are visible. The Ouémé River basin, located in Benin, exhibits such dynamics, undergoing rapid LULC changes due to agricultural expansion activities and urbanization (Olofintoye *et al.* 2022, Annan *et al.* 2024). These developments have significant effects on runoff patterns, water availability (Mbaye *et al.* 2015), and the basin's ability to provide ecosystem services in the long term and under extreme climate conditions. Awareness of these processes is important for the achievement of the Sustainable Development Goals (SDGs) 2 (zero hunger) and 6 (access to water and sanitation for all) for sustainable growth in agriculture.

The response of a watershed to rainfall events depends on its characteristics, such as soil properties, LULC, channel characteristics (length, roughness, width and depth), catchment size and shape, which define runoff generation and propagation as well as groundwater recharge (Mosavi *et al.* 2020). Thus, knowledge of how LULC change affects water balance is key to sustainable water resources management and ecosystem health. Such assessments cutting across short- and long-term periods provide further understanding of the temporal variations in the trends.

Previous research conducted in the Ouémé River basin have examined the effects of changes in LULC on water resources, including impacts on surface runoff, groundwater flow, and their local water management implications. For instance, Hiepe (2008) studied how LULC affect water balance and soil erosion in the upper Ouémé basin (Bétérou catchment) using an LULC map for the year 2000 from Landsat imagery and found that agricultural lands were more prone to soil erosion. Bossa *et al.* (2014) also modelled the effects of LULC change on land and water degradation in the Ouémé basin using LULC change scenarios from projected (2015–2029) socio-economic changes, specifically population growth, and a baseline LULC of 2003 Landsat imagery. They found that surface runoff and groundwater flow were more sensitive to LULC changes, while water yield and evapotranspiration were sensitive to climate change. Similarly, Hounkpè *et al.* (2019) derived LULC maps from projected socio-economic changes as forcing to assess the impact of LULC changes on flood characteristics in the Zou sub-catchment of the Ouémé basin using 2003 LULC from the RIVERTWIN project as a baseline. They found that expansion in agricultural lands and reduction in natural vegetation enhance the occurrence of floods in the Zou catchment, a sub-catchment of the Oueme basin. Abdulkadir *et al.* (2022) predicted water balance in the upper Ouémé basin (Bétérou catchment) from 1998 to 2007 using an LULC map from the Global Land Cover Characterization (GLCC) for April 1992 to March 1993 and observed that evapotranspiration was the highest component of water loss from rainfall while lateral flow was the least. Similar findings have been reported by Sintondji *et al.* (2014), who modelled water balance at the Savè outlet of the Ouémé basin using a LULC map of 2003 by the National Centre of Remote Sensing and Forest Cover Monitoring (CENATEL). Additionally, Olofintoye *et al.* (2022) predicted

CONTACT Ernestina Annan ernestinaannan39@gmail.com WASCAL Climate Change and Land Use, College of Engineering, KNUST Private Mail Bag, Kumasi, Ghana
Supplemental data for this article can be accessed online at https://doi.org/10.1080/02626667.2025.2516831

water balance values in the Bétérou catchment with the GLCC LULC map from April 1992 to March 1993 and compared simulated water balance values in 1998, 2008 and 2017. They observed an increase in precipitation and groundwater flow between 1998 and 2008, and a reduction between 2008 and 2017. Surface runoff and evapotranspiration, however, decreased over the period.

These studies either predicted water balance without considering LULC change, as they used constant maps, or used LULC scenarios derived from predicted socio-economic scenarios to assess changes in water balance in the future. The studies that used scenario-based LULC changes to assess water balance also did not explore the relationship between the LULC changes and changes in water balance nor the consistency of the relationship across different time periods. Such analysis has been a challenge due mostly to the unavailability of comprehensive LULC data for the entire basin and the lack of up-to-date hydrological and climate data (Giertz *et al.* 2006a, Bodjrènou *et al.* 2023). Therefore, there is a research gap regarding a full understanding of the effect of LULC changes on water balance, and the consistency of these effects across different time periods. However, such knowledge provides valuable insights into the hydrological response of the basin to environmental changes and future trends.

This study builds on existing research to evaluate the effects of LULC change on water balance across different periods in the Ouémé River basin. Changes in water balance components, including surface runoff, baseflow, lateral fow, total aquifer recharge, and evapotranspiration, are estimated using four LULC types with varying spatio-temporal proportions from a previous study (Annan *et al.* 2024) and observed climate data from the period 1998–2016. This study specifically seeks to (1) simulate water balance using four LULC maps; (2) estimate the relationship between changes in LULC types and corresponding changes in water balance components, using advanced linear regression analysis; and (3) examine the consistency and generalizability of the relationships across the different periods. The findings from this study provide valuable insights for understanding and making informed decisions regarding flood risk, sustainable water resources and ecosystem management within the region for improved food productivity and ecosystem health.

2 Materials and methods

2.1 Study area

The study was conducted in the Ouémé River basin, which is the largest basin in Benin, West Africa, covering about 43% of the country's land surface area, located between latitudes 6°30' and 10° 00'N, and longitudes 0°52' and 3°05'E, and has a tropical climate (Fig. 1). The figure also shows rainfall and temperature patterns across the basin, with annual rainfall and temperature values ranging between 900 and 1200 mm and between 25 and 30°C, respectively (Olofintoye *et al.* 2022). The basin has a total area of 49 280 km^2 and is characterized by diverse LULC types including croplands (mainly staples such as maize, millet, rice, cassava, yam, sorghum, etc.), plantations, forests, savanna areas or woodlands, urban areas and water bodies. Water in the basin is mainly used for household (drinking, cooking, bathing, etc.), industrial (e.g. sugar production by the *Sucrerie du Complant du Bénin*), transport and agricultural (crop and fish farming) purposes (Houssou *et al.* 2017).

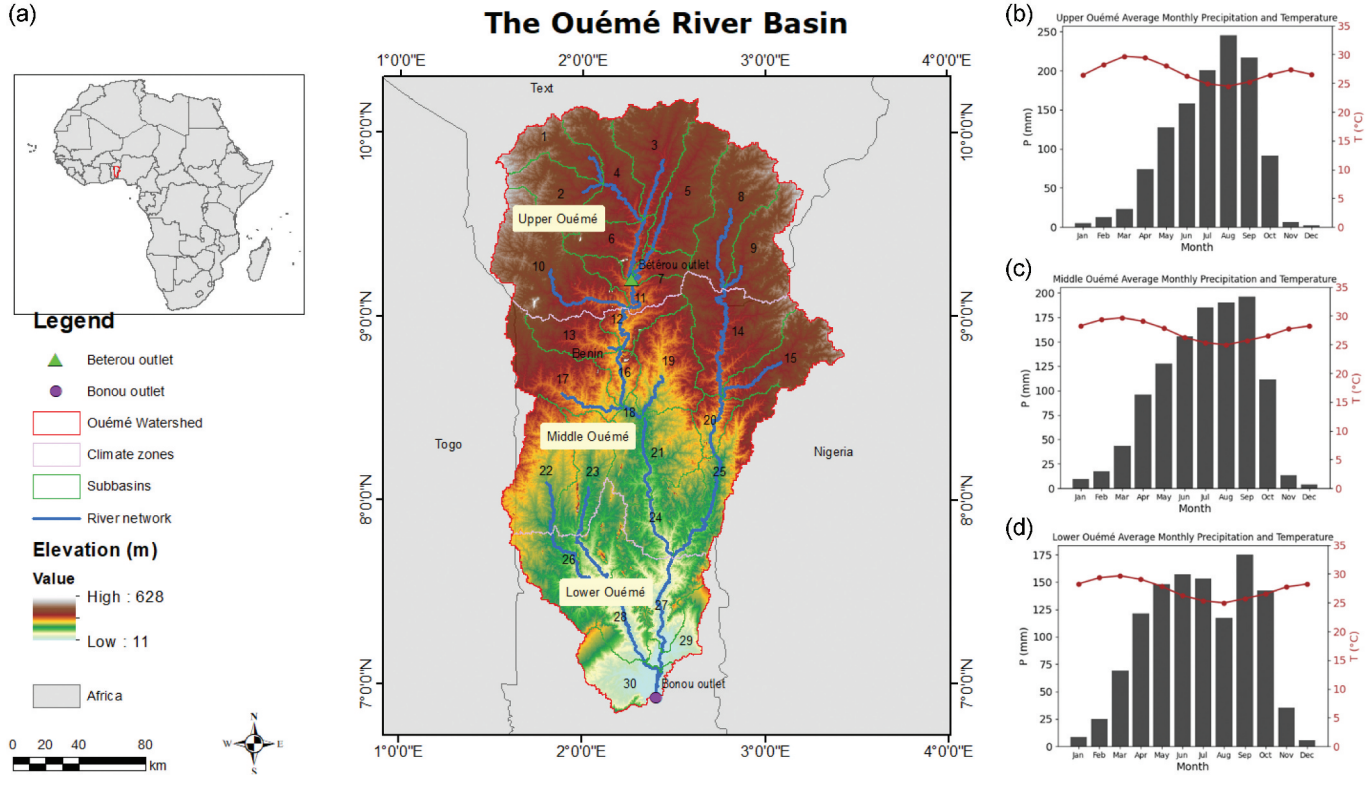

Figure 1. (a) Location of the Ouémé River basin in Benin, West Africa, showing the two sub-basins (Bétérou and Bonou outlets) used for the model simulation. The graphs on the right show the average monthly rainfall (1998–2016) for the Upper Ouémé with a unimodal rainfall regime (b) Middle Ouémé with a transitional rainfall regime (c) and Lower Ouémé with a bimodal rainfall regime (d) for the basin.

The land surface of the basin is slightly undulating with generally low relief, strongly fractured with seasonally waterlogged linear depressions (Bossa 2012). The upper portion of the Ouémé has a single rainy season which peaks in August (Fig. 1), while the lower portion has a bimodal rainfall system, a major rainy season which may begin in April/May and last through July, and a minor season which occurs between September and November. The middle portion exhibits characteristics of the upper and lower portions, with rainfall amounts in April to June higher than those in the upper portion but less than that in the lower portion. The Ouémé basin lies mainly in the Dahomeyen basement, which is composed of metamorphic and crystalline rocks with low permeability due to their solid and compact nature (Faure and Volkoff 1998). However, fractures in the rocks create pathways that enhance water infiltration. From the central to the northern parts of the basin are found tropical ferruginous soils (luvisols) which are formed through clay translocation and iron segregation (see Supplementary material, Fig. S1), while ferrallitic soils, which are highly weathered with high porosity, dominate in the south (Forbes 1973, Bossa 2012). The ferruginous soils, due to their hardened layers, promote surface runoff, while the ferrallitic soils support high infiltration but are often associated with lower nutrient retention due to leaching. There are also inland valleys in some parts of the basin where hydromorphic soils (gleysols) dominate, which have higher water retention but may result in waterlogging (Hiepe 2008).

The Bétérou outlet is located in the Upper Ouémé with a sub-catchment area of about 14 400 km^2 and elevations between 228 and 617 m (Olofintoye *et al.* 2022). Luvisols dominate that sub-catchment, and LULC consists of savanna areas, croplands, and urban areas. The Bonou outlet falls in the Lower Ouémé where streamflow from the Ouémé basin drains into the delta south of Bonou.

2.2 Hydrological modelling

2.2.1 The SWAT model set-up

The SWAT model is a continuous semi-distributed river basin simulation model, quasi-physically-based in nature, developed for predicting the long-term impacts of land management decisions on water, sediment, and agricultural chemicals in watersheds (Arnold *et al.* 1998). In SWAT, the catchment is first divided into sub-basins based on topography and then into hydrologic response units (HRUs), which are used to simulate runoff, sediment, and nutrient flows within the catchment (Fig. 2 describes the study's workflow). An HRU refers to the total area in a sub-basin with a particular LULC, management and soil type, capturing the diversity of LULC and soils in the sub-basins. Loadings from each HRU are calculated separately and summed together to obtain the total loadings from the sub-basin. HRUs are created by SWAT by defining a combination of LULC, soil and slope percentages, which the model uses to generate parameter characteristics for the sub-basins, such as the curve numbers. Threshold values of 2% LULC types, 10% soil type, and 20% slope levels were used to define the HRUs in this study. The lower threshold for LULC enables finer differentiation among areas that reflect the pattern of LULC changes over the sub-basin.

Due to data scarcity in the study region, the Hargreaves method for estimating potential evapotranspiration (PET) was applied (Hargreaves and Samani 1985). This method uses maximum and minimum temperature data, and latent heat of vaporization to estimate PET (Arnold *et al.* 1998). The Hargreaves method has shown similar performance to the more widely-used Penman-Monteith method in data-scarce regions, including parts of Benin and West Africa (Kilinzo *et al.* 2011, Adjei *et al.* 2023). SWAT calculates actual evapotranspiration values using the modified Ritchie (1972) criterion and simulates surface runoff using the modified SCS curve number (CN) method, which considers LULC, soil type, and antecedent moisture conditions. Additionally, lateral flow is estimated in SWAT by the kinematic method of Sloan and Moore, while baseflow is estimated with the linear storage approach (Arnold *et al.* 2013). The equation used for water balance simulation and the datasets used in this study are presented in Equation (1) and Table 1, respectively.

$$SW_t = SW_0 + \sum_{i-1}^{t}\left(R_{day} - Q_{surf} - ET_a - w_{seep} - Q_{gw}\right) \quad (1)$$

where:

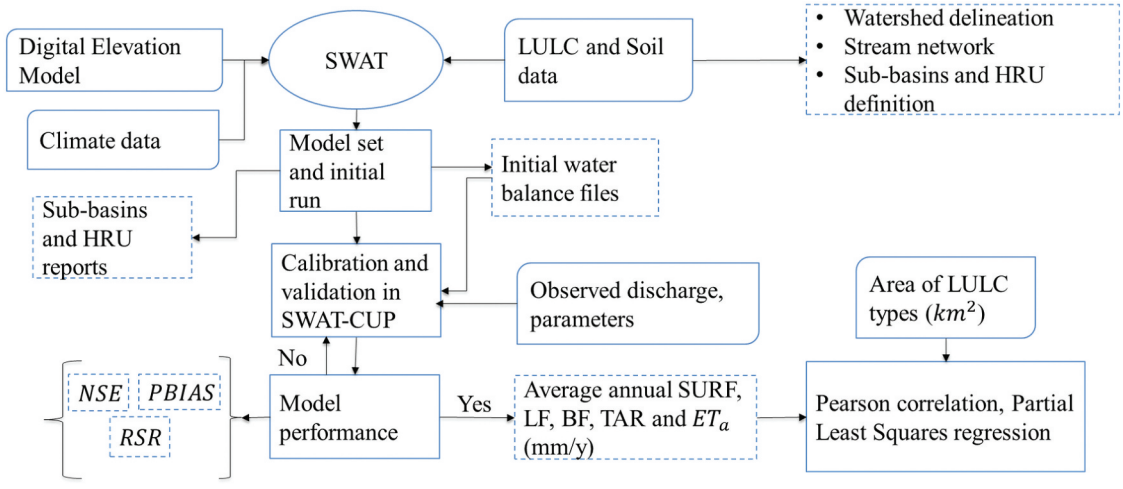

Figure 2. SWAT modelling and SWAT-CUP calibration and validation workflow for simulation and analysing surface runoff (SURF), lateral flow (LF), baseflow (BF), total aquifer recharge (TAR) and actual evapotranspiration (ET_a).

SW_t and SW_0 are the final and initial soil water content, respectively (mm H_2O)

R_{day} is the amount of precipitation on day i (mm H_2O)

Q_{surf} is the surface runoff on day i (mm H_2O)

ET_a is the actual evapotranspiration on day i (mm H_2O)

w_{seep} is the amount of water entering the vadose zone on day i (mm H_2O)

Q_{gw} is the amount of interflow on day i (mm H_2O)

2.2.2 Calibration, validation and parameter sensitivity analysis in SWAT-CUP

SWAT input parameters related to soil, LULC (Fig. 3 shows LULC maps for 1986, 2000, 2015 and 2023), and channel characteristics of the basin were generated following the initial model run (Table 2). From these, 16 parameters were selected for calibration and validation based on their significant impact on hydrology, soil properties, and land use, as identified in previous studies (Odusanya *et al.* 2021) and the SWAT documentation (Neitsch *et al.* 2002). The SWAT-Calibration and Uncertainty Program (CUP) was used to calibrate and validate the SWAT model for the basin.

Table 1. Datasets applied in this study.

Data type	Source	Resolution
Digital elevation model (DEM)	Shuttle Radar Topography Mission (SRTM)	30 m
Land cover maps (Fig. 3)	Annan *et al.* 2024)	30 m
Daily precipitation and temperature (1998–2016)	ERA5 Land (Rauch *et al.* 2024)	
Soil map	FAO soil database	1 km
Measured discharge	DGEau, Benin	

The SWAT model was calibrated first at Bétérou (upstream) and then at Bonou (downstream) with observed discharge data from 2000–2002 and the 2000 LULC map, utilizing the period 1998–1999 for model warmup. This calibration method was applied because the Bétérou outlet (9°11'56"N, 2°16'50"E) contributes directly to Bonou outlet (6°54'35"N, 2°26'35"E) as outlined in the SWAT-CUP user manual (Abbaspour 2015). After calibration at Bétérou, final parameter ranges were then used to initialize calibration at Bonou. The SUFI-2 (Sequential Uncertainty Fitting – 2) algorithm was employed, which uses the Latin hypercube sampling (LHS) method to simulate discharge. During the calibration process, SWAT approximates the total uncertainty by computing the 95% prediction uncertainty (95 PPU) between the 2.5% and 97.5% ranges of the cumulative distribution of the predicted discharge. The parameter uncertainty range is initially broader and is progressively narrowed based on the objective function while ensuring that most of the observed discharge points fall within the 95 PPU band (Abbaspour 2015). The p-factor and r-factor values are used to assess the uncertainty in the calibration and validation. The p-factor indicates the fraction of observed data that falls within the 95 PPU range, with values between 0 and 1. Values closer to 1 indicate more of the observed data falls within the 95 PPU, denoting that most of the

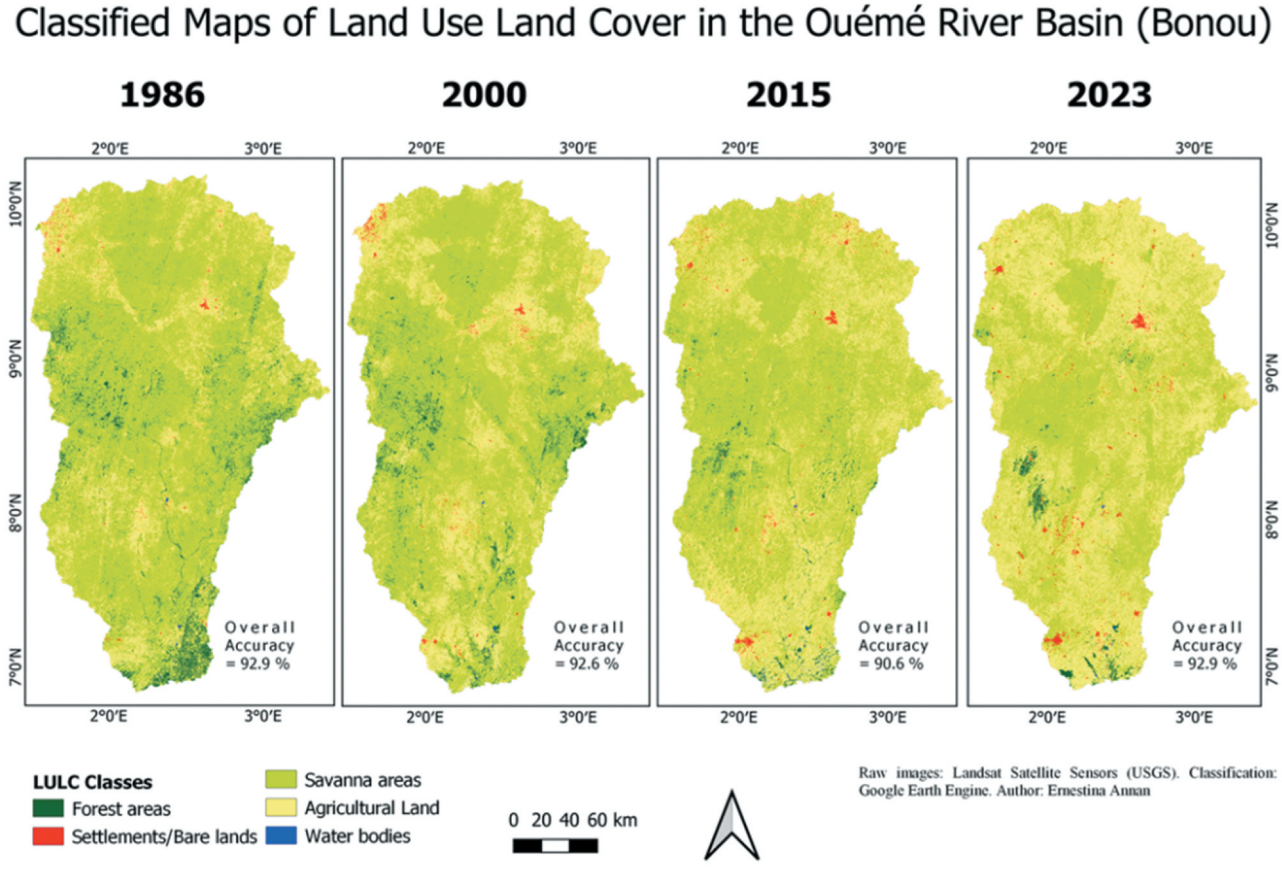

Figure 3. LULC maps for water balance simulation, from Annan *et al.* (2024) with permission from the authors, showing diminishing natural vegetation and increasing agricultural and urban areas over time.

Table 2. SWAT parameters used for calibration and validation.

SN	Parameter name	ID	Initial minimum value	Initial maximum value	Final minimum value	Final maximum value
1	Initial SCS runoff curve number for moisture condition II factor	CN2	−0.2	0.2	0.06	0.15
2	Baseflow alpha factor (days)	ALPHA_BF	0	1	0.05	0.50
3	Groundwater delay (days)	GW_DELAY	30	450	376.24	425.47
4	Threshold depth of water in shallow aquifer for return flow to occur (mm)	GWQMN	0	4950	3527.47	4101.76
5	Soil evaporation compensation factor	ESCO	0	1	0.55	0.74
6	Plant evaporation compensation factor	EPCO	0	1	0.52	0.84
7	Groundwater revap coefficient	GW_REVAP	0.02	0.2	0.09	0.11
8	Threshold depth of water in shallow aquifer for revap to occur (mm)	REVAPMN	20	450	108.90	134.21
9	Manning coefficient for main channel	CH_N2	−0.01	0.3	0.09	0.10
10	Effective hydraulic conductivity in main channel (mm/h)	CH_K2	−0.01	450	111.70	133.36
11	Maximum depth of soil profile (mm)	SOL_ZMX	20	3450	1818.63	1902.63
12	Soil depth (mm)	SOL_Z	20	3450	1152.90	1896.69
13	Moist bulk density (Mg/m^3 or g/m^3	SOL_BD	0.9	2.5	0.38	0.48
14	Available water capacity of soil layer (mm H_2O/mm soil)	SOL_AWC	0	1	0.46	0.83
15	Saturated hydraulic conductivity (mm/h)	SOL_K	0	9.503	0	9.50
16	Maximum canopy storage (mm H_2O)	CANMX	10	95	1.38	2.27

uncertainty in the observed data is accounted for. The r-factor describes the thickness of the 95 PPU, with lower values indicating a narrower uncertainty range (less uncertainty) and good model precision. The selected parameters were propagated and updated until the values of simulated discharge were very close to the observed discharge, indicated by satisfactory objective function values as outlined by Moriasi *et al.* (2007). Observed discharge data from 2003–2008 was used for validation.

The model was evaluated using the commonly used model performance metrics, including Nash-Sutcliffe efficiency (NSE), coefficient of determination (R^2), percent bias (PBIAS), and RMSE-observations standard deviation ratio (RSR), according to the ranges recommended by Moriasi *et al.* (2007) and presented in Table S2 in the Supplementary material. The metric equations are provided in the Appendix.

2.3 Analysis of LULC change impact on water balance

Four LULC maps derived from Landsat images of the dry season (30 m resolution) were obtained from the study of Annan *et al.* (2024) for the years 1986, 2000, 2015, and 2023. The maps were characterized by varying quantities of forest areas, settlements/bare lands, savanna areas, water bodies and agricultural lands (see Supplementary material, Table S1), which represent key ecosystems in West Africa. These LULC classes reflect in general the natural and human-induced changes in the land influencing the hydrological cycle. SWAT LULC groups 'FRSD' (Forest Deciduous), 'URBN' (Urban area), 'RNGB' (Range-Brush), and 'AGRL' (Agricultural Land-Generic) together with soil hydrologic groups were used to define the CN values for forests, settlements/bare lands, savanna areas, and agricultural lands, respectively (Hiepe 2008, Hounkpè 2016). Though challenged by the lack of detailed spatial data, such as specific vegetation or crops, these general SWAT LULC groups helped capture the overall influence of agricultural management/expansion and urbanization on hydrological processes in the basin. Each LULC map was used to simulate water balance for three distinct periods – 1998–2008, 2008–2016, and 1998–2016 – without changing climate and soil data inputs. The isolation of LULC as a primary variable aims to better understand how changes in LULC alone, such as deforestation, agricultural expansion and urbanization, affect hydrological processes in the basin. This approach resulted in 12 sets of water balance outputs, combining each LULC map with each time period, enabling the assessment of temporal variations in the impacts of LULC change on water balance components. Key water balance components considered in this study include average annual surface runoff (mm), total aquifer recharge (mm), baseflow (mm), lateral flow (mm), and actual evapotranspiration.

The 1986 LULC map (LM1) depicts 23.3% agricultural land, 0.6% settlements/bare lands, 6.3% forest areas, and 69.7% savanna areas. The second map of 2000 (LM2) has fewer forest and savanna areas (4.3% and 65.9%, respectively), and more settlements/bare lands and agricultural lands (0.8% and 29.0%, respectively). The 2015 map (LM3) is characterized by a further reduction in forest and savanna areas (2.4% and 58.3%, respectively), and more expansion in agricultural lands and settlements/bare lands (38.0% and 1.2%). By 2023 (LM4), forest areas had diminished to 1.4% and savanna areas to 45.7%, while agricultural lands had expanded to 51.3% and settlements/bare lands to 1.6%. Overall, the LULC changes across the maps depict declining natural vegetation and expanding agricultural lands and urban areas (refer to Table S1 in the Supplementary material).

To explore the relationship between changes in LULC and the average annual water balance values from the SWAT model, statistical analyses were applied. Firstly, the distribution of the simulated water balance component was tested for normality using the Shapiro-Wilk test, and a Quantile-Quantile (Q-Q) plot was used to visualize the results.

2.3.1 Correlation analysis

Pearson's pair-wise correlation was applied to examine the strength and direction of the connection between the areas of the LULC types and average annual surface runoff (mm), lateral flow (mm), baseflow (mm), and total aquifer recharge (mm). This was conducted across the three time periods, with the area of the LULC types of each map (refer to Table S1 in the Supplementary material) and the absolute amounts of the water balance

components simulated per map (see Supplementary material, Fig. S2) input. Values closer to 1 indicate strong correlations while values closer to 0 indicate weaker correlations.

2.3.2 Independent t-test

The difference between the mean water balance components simulated for the 1986 and 2023 LULC maps was assessed for significance using an independent t-test. The test was performed at the 5% significance level (95% confidence interval). The independent t-test's null hypothesis assumes that the mean values of the water balance components for the 1986 map are equal to those for the 2023 map. Suppose the test produces a p value of less than .05. In that case, the null hypothesis is rejected, meaning there is a statistically significant difference between the mean water balance values of the two maps. This would suggest there is evidence that those water balance components have been significantly influenced by the changes in LULC that occurred between 1986 and 2023. A higher magnitude of the test statistic (t) signifies a larger difference between the means of the water balance components relative to the variability in the data, while a smaller value indicates higher variability in the data, making it harder to differentiate between the two means.

2.3.3 Test for predictability and generalizability of trends

Partial least squares (PLS) regression was applied to model the relationship between the LULC types and water balance components for each simulation period, considering the high multicollinearity within the LULC types. PLS is a supervised learning method that generates a set of latent variables (linear combinations of the original predictors – LULC types) closely related to the response variables (water balance components), hence addressing collinearity and reducing dimensionality. The latent variables are created such that they properly capture the contribution of the predictor variables while adequately explaining the variance in the response variables (Pirouz 2006, Abdi 2010). PLS is appropriate when there are strongly correlated predictors, multiple response variables and few sample points, where ordinary linear regression fails. PLS regression coefficients are produced, which quantify the expected change in water balance components for a unit change in each of the LULC types. This provides an understanding of how much the LULC types influence water balance in the basin (Geladi and Kowalski 1986, Aladejana *et al.* 2018).

The calibrated and validated SWAT model for the basin using observed discharge data from 1998–2008 was used to predict discharge for 2008–2016 in SWAT (where observed discharge data was absent). Four distinct PLS models were developed to evaluate different scenarios. In the first model (PLS1), the relationship between LULC types and water balance components was modelled for each simulation period. The input for PLS1 was the areas of the LULC maps (LM1, LM2, LM3 and LM4) and their corresponding amounts of the water balance components for the three periods. The second PLS model (PLS2) used data (area of LULC types and corresponding water balance) from the period 1998–2008 as training data to predict water balance components for the subsequent simulation periods of 2008–2016 and 1998–2016. In the third PLS model (PLS3), data from 2008–2016 served as the training set, and the model was used to predict water balance components for the periods 1998–2008 and 1998–2016. The fourth PLS model (PLS4) used data from 1998–2016 as the training data to predict water balance components for the periods 1998–2008 and 2008–2016. The performance of these models, PLS2, PLS3 and PLS4, in terms of how well they could predict water balance components for these test periods, was used to test the predictability, consistency and generalizability of the impact of LULC change on the different water balance components.

The performance of the PLS models was assessed using mean absolute error (MAE), RMSE, and R^2. The PLS model expressions for predicting the response variables (water balance) from the predictors (LULC) are presented in Equation (2) and the Appendix (Abdi 2010).

$$\widehat{Y} = XB_{PLS} = XW\left(P^TW\right)^{-1}Q^T \quad (2)$$

where:

$\widehat{Y}$ is the predicted response variable (surface runoff, lateral flow, baseflow, actual evapotranspiration and total aquifer recharge)

X is the matrix of predictors (LULC types)

B_{PLS} is the matrix of regression coefficients estimated by the PLS model

W is the weight matrix that relates X to the latent scores T

$\left(P^TW\right)^{-1}$ rescales the weights in W to align with the variance captured in each component

Q is the matrix of the loadings for Y

P is the matrix of the loadings for X

The variable importance in projection (VIP) test was used to assess the importance of each LULC type in predicting the water balance components. A VIP value greater than or equal to 1 indicates high importance of the predictor variable in explaining the response variables.

3 Results

3.1 SWAT model calibration and validation

The uncertainty assessment of the calibration at Bétérou yielded a p-factor of 0.63 and an r-factor of 1.09, while validation results showed a p-factor of 0.54 and an r-factor of 1.19 (see Supplementary material, Fig. S4). At Bonou, the calibration produced a p-factor of 0.45 and an r-factor of 1.32, with validation values of 0.42 for the p-factor and 1.28 for the r-factor (Fig. 4 showing discharge plots). Generally, p-factor values above 0.5 and r-factor values below 1.5 are considered acceptable (Abbaspour 2015).

The calibration and validation performance at Bétérou and Bonou stations within the Ouémé River basin are summarized in Table 3. The calibration and validation demonstrated satisfactory performance as outlined by Moriasi *et al.* (2007), indicating good agreement between the simulated and observed discharge at both stations. The negative PBIAS values obtained at both stations (Table 4) are indicative of a general overestimation of discharge by the model, although they are within acceptable limits (see Supplementary material, Table S2).

3.2 LULC change impact on water balance components

The influence of agricultural lands, forest areas, savanna areas, and settlements/bare lands on water balance were examined at

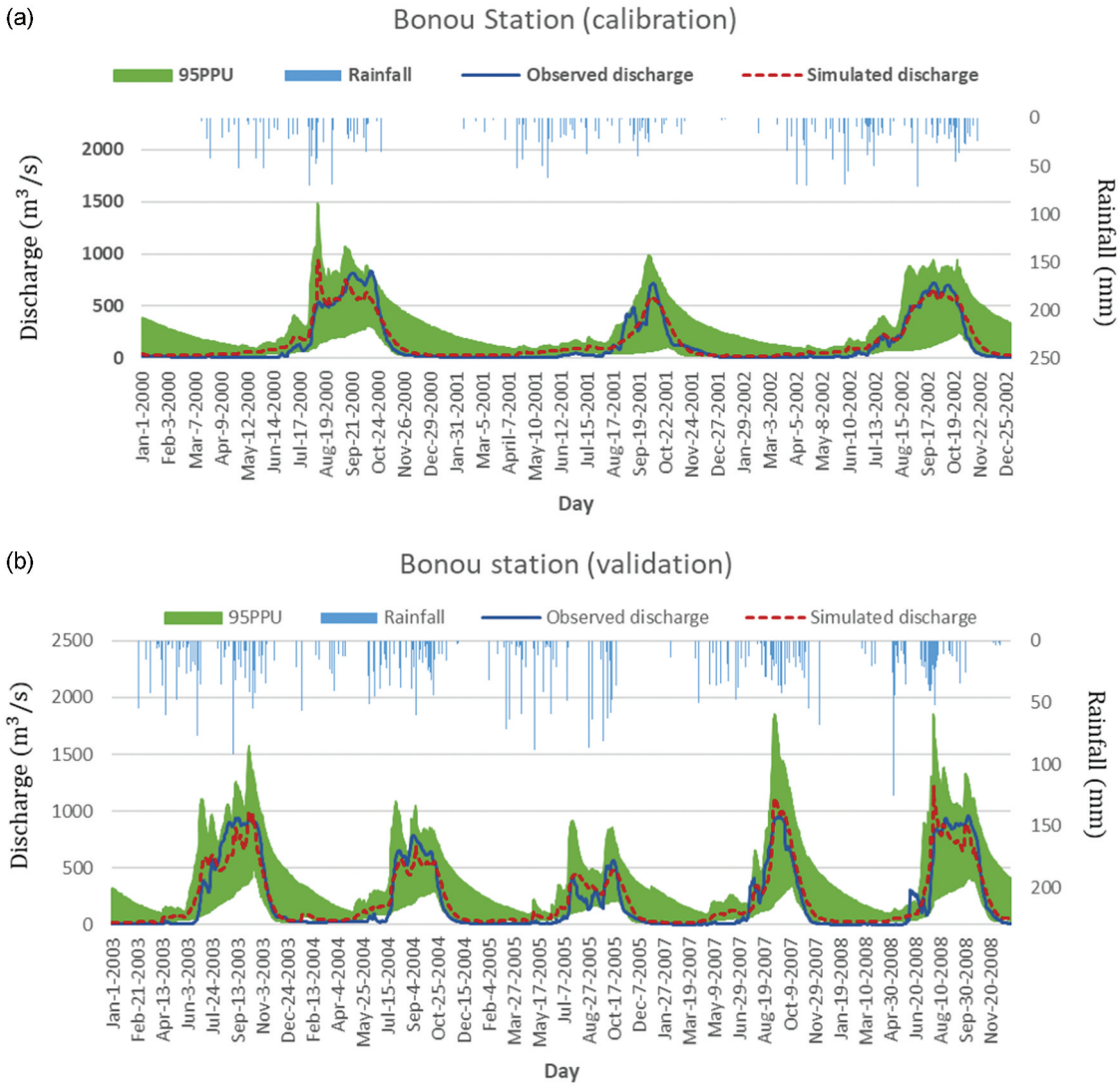

Figure 4. Calibration (a) and validation (b) results at Bonou Station (outlet), showing simulated versus observed discharge, rainfall and the 95 PPU range.

Table 3. Performance of the SWAT model calibration and validation at Bétérou and Bonou stations.

Station	Model performance	NSE	RSR	PBIAS	R^2	KGE
Bétérou (upstream)	Calibration (1998–2002)	0.82	0.42	−6.6	0.85	0.74
	Validation (2003–2008)	0.81	0.43	−14.4	0.83	0.74
Bonou (downstream)	Calibration (1998–2002)	0.91	0.31	−12.8	0.92	0.82
	Validation (2003–2008)	0.89	0.33	−10.7	0.90	0.84

the basin scale using average annual values across the four LULC maps and periods (1998–2008, 2008–2016, and 1998–2016). The baseline values were determined from the earliest LULC map (1986) for each period, as a reference to assess water balance changes across the LULC maps. Water bodies constituted less than 0.01% of the basin area and exhibited irregular trends in change compared to other LULC types, hence its impact was deemed negligible and was excluded from the statistical analysis.

The proportions of average values of the water balance components showed that evapotranspiration accounted for the largest fraction of precipitation (57%) (Abdulkadir *et al.* 2022, Bodjrènou *et al.* 2023), followed by total aquifer recharge (approximately 27%). Lateral flow accounted for 10% and surface runoff about 5%, while baseflow showed varying proportions as illustrated in Fig. S1 in the Supplementary material.

Between maps LM1 (1986 LULC) and LM4 (2023 LULC), surface runoff increased by approximately 67%, while baseflow, lateral flow, actual evapotranspiration, and aquifer recharge decreased across all periods as shown in Table 4, which compares the change in LULC types with change in water balance components. For instance, for the 1998–2016 simulation, a reduction by approximately 2432 km^2 of forest and 11 867 km^2 of savanna areas, coupled with an increase by 534 km^2 in settlements/bare lands and 13 776 km^2 in agricultural lands, resulted in a 32 mm/year increase in surface runoff. Concurrently, reductions of 12, 6, 26, and 5.9 mm/year in baseflow,

Table 4. Percentage change in LULC, and corresponding change in water balance components between the LULC maps and across the three simulation periods (LM1: 1986 LULC map, LM2: 2000 LULC map, LM3: 2015 LULC map, LM4: 2023 LULC map).

	Change in LULC				Change in water balance				
		1998–2016 simulation							
LULC map	Forest areas (%)	Settlements/bare lands (%)	Savanna areas (%)	Agricultural lands (%)	Surface runoff (%)	Baseflow (%)	Lateral flow (%)	Total aquifer recharge (%)	Actual ET (%)
LM1-LM2	−32.57	36.30	−5.53	24.58	15.30	−4.23	−1.96	−1.61	−0.03
LM2-LM3	−44.42	61.94	−11.52	30.69	16.13	−4.51	−1.66	−1.26	−0.43
LM3-LM4	−41.88	33.77	−21.68	35.08	24.54	−4.45	−2.02	−5.21	−0.42
LM1-LM4	−78.22	195.25	−34.53	119.93	66.76	−21.77	−5.54	−7.90	−0.88
1998–2008 simulation									
LM1-LM2	−32.5 7	36.30	−5.53	24.58	14.59	−1.52	−1.90	−1.46	0.06
LM2-LM3	−44.42	61.94	−11.52	30.69	15.49	−0.40	−1.58	−1.20	−0.45
LM3-LM4	−41.88	33.77	−21.68	35.08	24.70	−6.26	−1.98	−3.44	−0.40
LM1-LM4	−78.22	195.25	−34.53	119.93	65.03	−8.06	−5.36	−5.99	−0.79
2008–2016 simulation									
LM1-LM2	−32.57	36.30	−5.53	24.58	15.89	3.69	−2.05	−1.69	0.01
LM2-LM3	−44.42	61.94	−11.52	30.69	16.63	−6.11	−1.78	−1.41	−0.43
LM3-LM4	−41.88	33.77	−21.68	35.08	24.01	−7.49	−2.10	−3.43	−0.42
LM1-LM4	−78.22	195.25	−34.53	119.93	67.61	−9.94	−5.81	−6.40	−0.84

lateral flow, total aquifer recharge, and actual evapotranspiration, respectively, were observed.

The increase in surface runoff between LULC maps LM3 (2015 LULC) and LM4 (2023 LULC) was higher, compared to the increase between LM1 and LM2, and between LM2 and LM3, despite the smaller number of years between LM3 and LM4. For the 1998–2016 simulation, for instance, surface runoff increased by 15.6 mm/year between LM3 and LM4, as compared to 7.28 and 8.6 mm/year increase between LM1 and LM2, and between LM2 and LM3, respectively. At the same time, a greater reduction was observed in baseflow, lateral flow and total aquifer recharge between maps LM2 and LM3 than between LM3 and LM4. This trend was similar across the other two simulation periods, except for baseflow which had much higher reduction over the 16-year simulation period (2.4, 2.5, and 7.5 mm/year between LM1 and LM2, LM2 and LM3 and LM3 and LM4, respectively) than across the two 8-year simulation periods (0.27, 0.07, 1.09; and 0.74, 1.3, and 1.5 mm/year). The Q-Q plots (see Supplementary material, Fig. S5) indicated that these distributions were approximately normal.

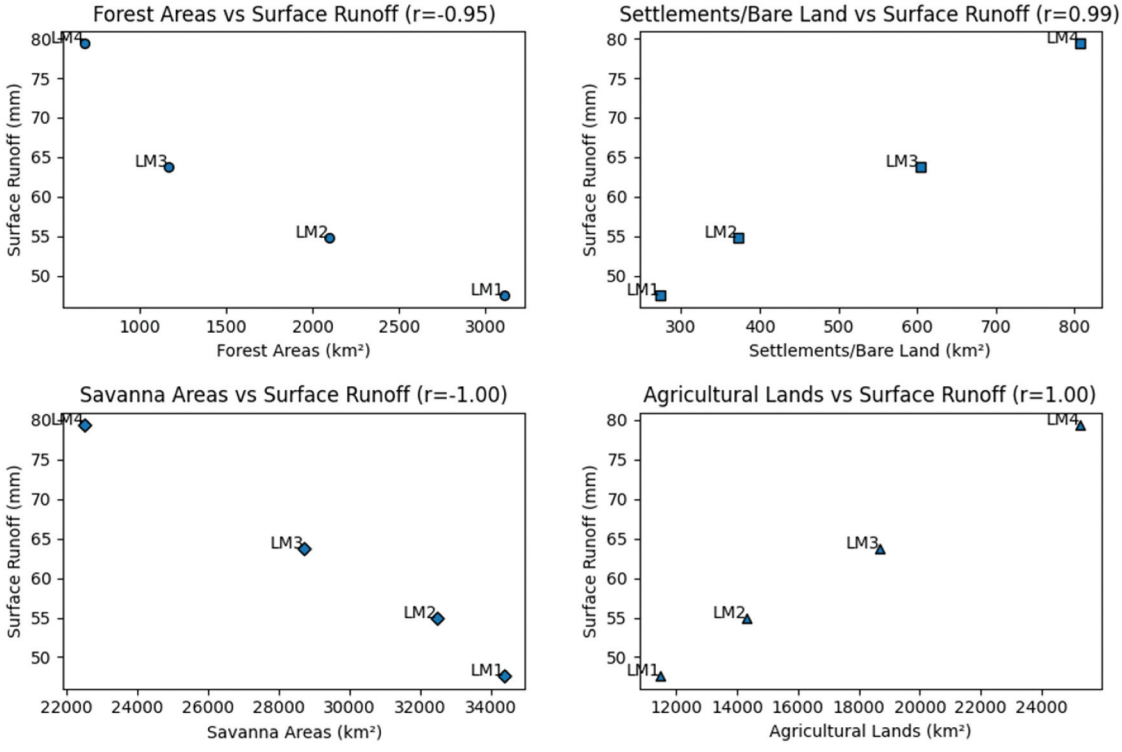

Figure 5. Correlation between average annual surface runoff and area of forests (a) settlements/bare lands (b) savanna areas (c) and agricultural lands (d) showing their correlation coefficients (r).

3.2.1 Correlation between LULC and water balance

The analysis revealed a strong positive correlation between the area of forests and the amount of baseflow, lateral flow, total aquifer recharge, and actual evapotranspiration, but a strong negative correlation with the amount of surface runoff as illustrated in Fig. 5, which shows the correlation between surface runoff and the LULC types. This was similar to savanna areas. In contrast, the area of agricultural lands had a strong positive correlation with the amount of surface runoff generated, and a negative correlation with baseflow, lateral flow, total aquifer recharge and evapotranspiration, as did settlements/bare lands. These findings indicate a substantial connection between changes in LULC and changes observed in the water balance components. Furthermore, these correlation results indicate that increases in agricultural and settlements/bare land together with loss of forests and savanna through anthropogenic activities such as deforestation, expansion of farmlands and urbanization, were associated with increased surface runoff and reduced baseflow, aquifer recharge, lateral flow and actual evapotranspiration. This correlation was consistent across the three simulated periods, as indicated by the correlation coefficients plotted in Fig. 6, emphasizing the significant effect of LULC changes on the region's hydrology.

3.2.2 Independent t-test analysis

Results from the independent t-test analysis revealed a statistically significant difference ($p < .05$) between mean surface runoff, lateral flow and total aquifer recharge for LM1 and those for LM4. The mean surface runoff of the LM4 map (80.77 mm/year) was significantly higher than that of the LM1 map (48.51 mm/year) with a difference of -32.26 ± 7.99 mm (Table 5). The t-statistic for surface runoff (−12.88) was notably higher than those for lateral flow (3.15) and total aquifer recharge (2.9), indicating a strong sensitivity of surface runoff to changes in LULC across the three simulated periods.

Conversely, the mean lateral flow obtained for the LM4 LULC map (109.44 mm/year) was significantly lower than that obtained for the LM1 map (115.90 mm/year). Mean total aquifer recharge was significantly higher in the LM1 LULC map (328.61 mm/year) compared to the LM4 map (306.36 mm/year). These findings suggest that the decrease in forest and savanna areas between LM1 and LM4 LULC maps together with the expansion of settlements/bare lands and agricultural lands led to a considerable increase in surface runoff and a reduction in subsurface flow and evapotranspiration in the basin.

3.2.3 PLS regression analyses

The PLS regression analyses provided significant insights. The loading patterns of the predictor variables (area of forest areas, settlements/bare lands, agricultural lands, and savanna areas), represented as X, and the response variables (average annual surface runoff, baseflow, lateral flow, total aquifer recharge, and actual evapotranspiration), represented as Y, showed consistent trends across the periods (Fig. 7). Components 1 and 2 are the latent variables onto which predictor and response variables are projected to reduce dimensionality. A higher loading value of a variable in a component means that this variable is strongly associated with that component, indicating that this variable plays an important role in explaining the relationship between the predictor and response variables.

Component 1 was associated strongly with a reduction in forest and savanna areas, together with an expansion of settlements/bare lands and agricultural lands (Fig. 7). This corresponds with a decrease in baseflow, lateral flow, total aquifer recharge, and actual evapotranspiration, but an increase in surface runoff. The second component displayed a strong association with forest expansion and a reduction in savanna areas, and a weaker correlation with increases in agricultural and settlements/bare lands. This corresponded with a reduction in baseflow, total aquifer recharge, and actual

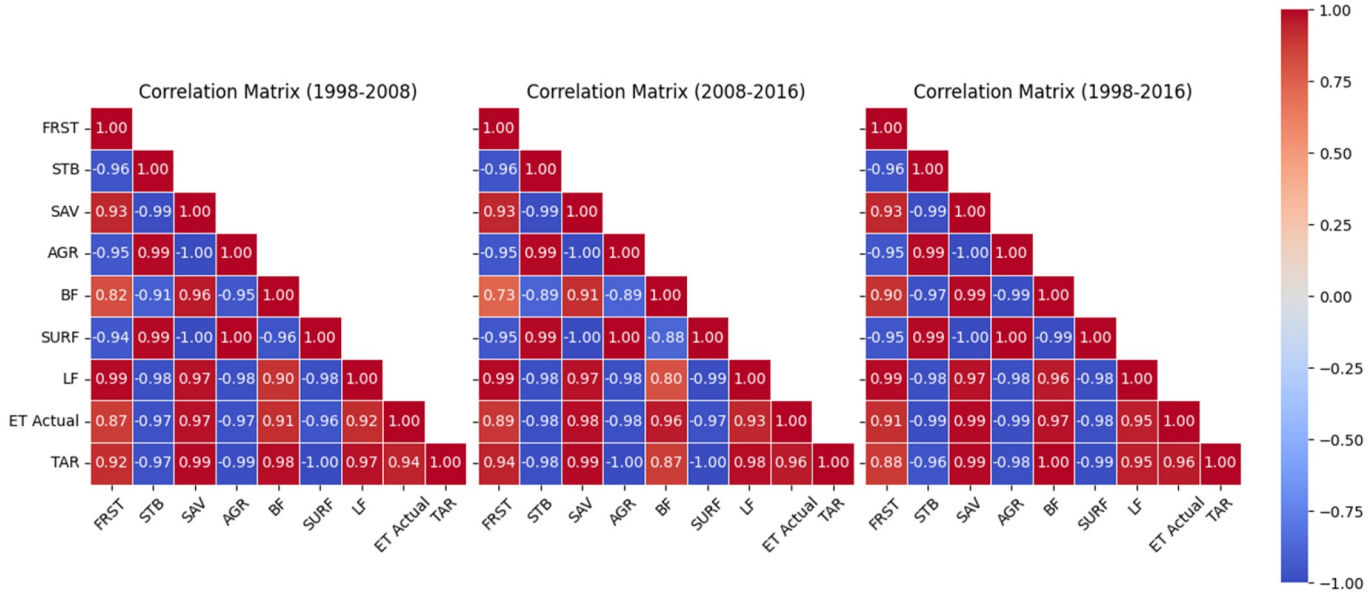

Figure 6. Correlation between LULC types, forest areas (FRST), settlements/bare lands (STB), savanna areas (SAV), agricultural lands (AGR), and water balance components, surface runoff (SURF), baseflow (BF), lateral flow (LF), actual evapotranspiration (ET actual) and total aquifer recharge (TAR).

Table 5. Results of independent t-test analysis to test for statistical significance of the difference between mean water balance for LM1 (1986) and LM4 (2023) LULC maps.

Water balance component	t-statistic	*p* value	Difference ± 95% CI
Surface runoff (mm/year)	−12.88	0.001	−32.26 ± 7.99
Lateral flow (mm/year)	3.15	0.034	6.46 ± 5.74
Total aquifer recharge (mm/year)	2.90	0.044	22.25 ± 21.37
Baseflow (mm/year)	0.34	0.753	5.27 ± 45.21
Actual evapotranspiration (mm/year)	0.29	0.788	5.60 ± 53.75

evapotranspiration, with a slight increase in lateral flow and surface runoff.

The values of R^2 obtained for PLS1 confirmed the correlation results, demonstrating a strong relationship between the LULC types and the water balance components ($R^2 \geq 0.85$) across the three time periods. It signifies that LULC changes were able to explain more than 85% of the variances in surface runoff, baseflow, lateral flow, aquifer recharge and evapotranspiration patterns. The RMSE of the PLS1 model of all the water balance components ranged between 0.27 and 2.55 mm/year. Among the water balance components, actual evapotranspiration prediction had the highest RMSE value, from the 1998–2016 simulation, while lateral flow had the lowest value, from the 1998–2008 simulation.

The results from PLS1 model coefficients show that a unit (1 km^2) increase in settlements/bare lands led to the highest influence (14.7×10^{-3} mm/year) on surface runoff, increasing it consistently across the three time periods in component 1. Agricultural lands also increased runoff (0.6×10^{-3} mm/year), while forest (-13.1×10^{-3} mm/year) and savanna areas (-0.7×10^{-3} mm/year) reduced it (where other LULC types are equal to zero) (Table 6). In contrast, lateral flow, baseflow, aquifer recharge, and actual evapotranspiration increased with a unit increase in forest and savanna areas, while the expansion of settlements/bare lands and agricultural lands decreased them. These trends were consistent across the different time periods. Overall, changes in the area of settlements/bare lands, followed by changes in forest areas, had the highest regression coefficients from model predictions of surface runoff, lateral flow, baseflow, total aquifer recharge, and actual evapotranspiration, indicating that they are key predictors of these water balance components in the basin. Component 2 showed inconsistent relationships between forest areas and water balance, but settlements/bare lands and agricultural lands consistently increased runoff and reduced subsurface flow, aquifer recharge and actual evapotranspiration. Savanna areas reduced surface runoff and increased subsurface flows and aquifer recharge.

PLS2 was trained on data from the 1998–2008 simulation and gave R^2 values of 0.800 and 0.988 for predicted surface runoff for the periods 2008–2016 and 1998–2016, respectively. Lower R^2 values were obtained for lateral flow, baseflow, total aquifer recharge, and actual evapotranspiration ($R^2 = 0$). This trend was similar for the PLS3 and PLS4 models. PLS3 trained on 2008–2016 simulation data gave R^2 of 0.749 and 0.847 for the period 1998–2008 and 1998–2016, respectively – predictions of surface runoff. Finally, PLS4, trained on 1998–2016 simulation data, also produced strong predictive power, with R^2 values of 0.987 and 0.869 when used to predict surface runoff of the 1998–2008 and 2008–2016 periods. Prediction of lateral flow for 1998–2008 also gave a high R^2 value of 0.991. The predictions of the other water balance components showed low predictability ($R^2 = 0$).

The VIP values (see Supplementary material, Fig. S3) revealed varying degrees of influence of the LULC types on the different water balance components with similar trends across all three periods. For surface runoff, aquifer recharge and actual evapotranspiration, changes in savanna areas, agricultural lands, and settlements/bare lands had greater importance compared to changes in forest areas (VIP scores ≥ 1). Lateral flow was most affected by changes in settlement/bare lands and forests areas, while baseflow was more influenced by changes in savanna areas, agricultural lands and forest areas.

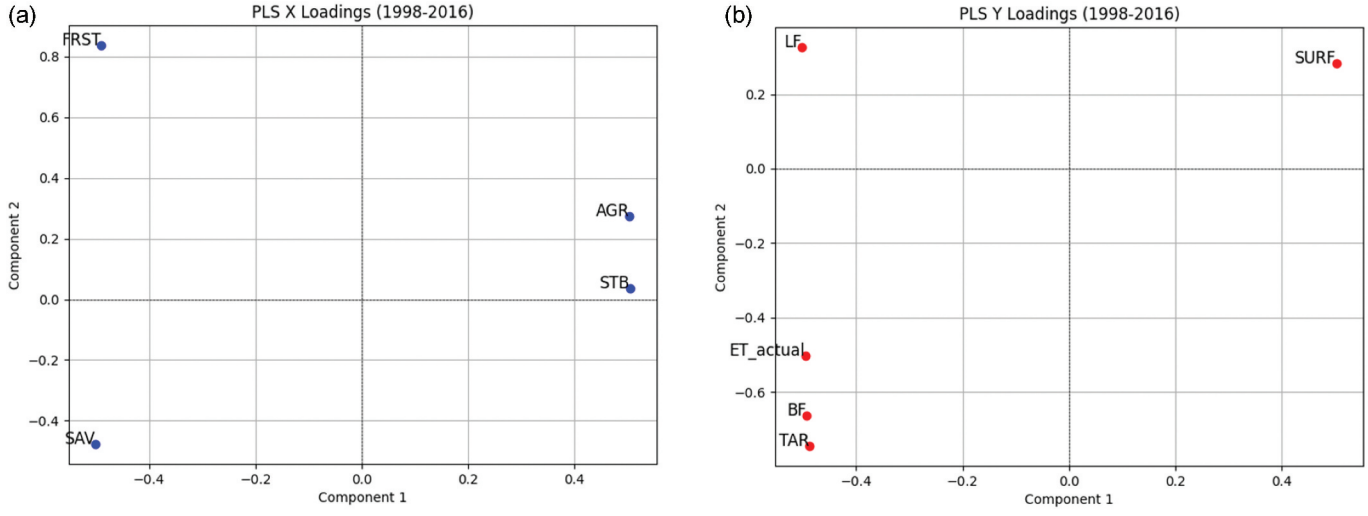

Figure 7. Plot of X loadings (a) and Y loadings (b) for the PLS model trained on results from the simulation period 1998–2016. X variables are forest areas (FRST), settlements/bare lands (STB), savanna areas (SAV) and agricultural lands (AGR); and Y variables are surface runoff (SURF), lateral flow (LF), baseflow (BF), total aquifer recharge (TAR) and actual evapotranspiration (ET_actual). Component 1 and 2 are latent variables (spaces) the PLS model generates from projecting the variances in X and Y.

Table 6. PLS1 coefficients (from component 1) of the LULC types showing the contribution to influencing changes in the various water balance components. FRST: forest areas, STB: settlements/bare lands, SAV: savanna areas, AGR: agricultural lands.

		PLS1 coefficients of LULC types per water balance component				
Period	LULC type	Surface runoff (10^{-3} mm/year)	Lateral flow (10^{-3} mm/year)	Baseflow (10^{-3} mm/year)	Total aquifer recharge (10^{-3} mm/year)	Actual evapotranspiration (10^{-3} mm/year)
1998–2008	FRST	−2.963	0.612	0.123	1.788	0.530
	STB	13.951	−2.740	−0.614	−8.463	−2.644
	SAV	−0.645	0.124	0.030	0.395	0.121
	AGR	0.563	−0.109	−0.026	−0.344	−0.105
	Intercept	67.61	109.86	16.90	305.91	641.87
	R^2	0.987	0.986	0.851	0.966	0.918
	RMSE	1.301	0.269	0.210	1.290	0.631
2008–2016	FRST	−3.344	0.694	0.202	2.054	0.596
	STB	15.651	−3.105	−1.100	−9.617	−2.938
	SAV	−0.721	0.140	0.052	0.446	0.135
	AGR	0.630	−0.124	−0.044	−0.390	−0.117
	Intercept	73.98	113.95	19.03	323.55	689.07
	R^2	0.992	0.986	0.760	0.978	0.942
	RMSE	1.162	0.303	0.489	1.176	0.583
1998–2016	FRST	−3.081	0.634	1.150	2.373	0.606
	STB	14.468	−2.834	−5.548	−11.494	−2.945
	SAV	−0.667	0.128	0.261	0.544	0.135
	AGR	0.583	−0.113	−0.226	−0.471	−0.117
	Intercept	68.905	109.72	49.08	313.101	667.41
	R^2	0.989	0.986	0.950	0.961	0.932
	RMSE	1.223	0.278	1.038	0.474	2.548

4 Discussion

4.1 Model calibration and validation

The SWAT model calibration and validation at the upstream Bétérou and downstream Bonou stations yielded satisfactory results, with higher values of NSE (0.81–0.91), PBIAS (−6.6 – (−14.4)), and R^2 (0.83–0.92) (Moriasi *et al.* 2007). Although negative PBIAS values indicated some overestimation, they remained within acceptable limits. This suggests that though the model captures the basin's overall hydrological processes well, there are some discrepancies, which could be attributed to the uncertainties in the input (e.g. climate data) and calibration procedure (Odusanya *et al.* 2021).

At Bétérou, the p-factor values of the model calibration and validation were above the recommended threshold (0.50), indicating that more than half of the observed discharge data fell within the predicted uncertainty range, suggesting a reasonable predictive capacity of the model. On the contrary, Bonou had p-factor values slightly below the threshold, signalling that more than half of the uncertainty in the observed discharge were not well captured by the calibration, due possibly to low quality of input data or mode parametrization (Fisher *et al.* 2018, Hounkpè and Diekkrüger 2018). The r-factor values obtained at Bonou exceeded 1.2, reflecting a wider uncertainty band, a common challenge when simulating hydrological processes in complex tropical basins (Bossa *et al.* 2014, Saddique *et al.* 2020). Such findings suggest that further calibration efforts, incorporating higher-resolution satellite data or refining key parameters, may reduce this uncertainty. In addition, other hydrological processes can be considered to address the uncertainty and improve the model parametrization, such as the actual evapotranspiration or the vegetation growth coupled with an evapotranspiration estimation (Odusanya *et al.* 2021, Merk *et al.* 2024).

4.2 Sensitivity of water balance components to changes in LULC

Diminishing forest and savanna areas, together with the expansion of agricultural and settlements/bare lands through anthropogenic activities such as expansion of farmlands for food production, deforestation and urbanization, strongly correlated with an increase in surface runoff and reduction in lateral flow, baseflow, aquifer recharge and actual evapotranspiration. This is attributable to the dense vegetation in forest and savanna areas that intercept rainfall and slow runoff, and the dense root system that increases infiltration rates compared to agricultural and settlements/bare lands. The results from the independent t-test indicated significant differences between the mean surface runoff, lateral flow, and total aquifer recharge from LM1 (1986 LULC map) and the mean values from LM4 (2023 map). This demonstrates that these water balance components are very sensitive to LULC changes. Though the difference in baseflow and actual evapotranspiration showed no statistical significance, the results still reflect important ecological effects (White *et al.* 2014), suggesting that these components are affected by LULC changes, though the changes may be more graduate or less immediate. These findings corroborate studies in the Upper and Lower Ouémé basin which found that degraded and agricultural areas experienced lower soil infiltration capacity, resulting in higher runoff (Hounkpè and Diekkrüger 2018, Abdulkadir *et al.* 2022, Osseni *et al.* 2022). The reduction in aquifer recharge and lateral flow emphasizes the need for conservative agriculture practices such as cover cropping and minimum tillage (Togbévi *et al.* 2022), to prevent the already low-fertility ferruginous soils from further degrading and affecting food productivity (Dossou *et al.* 2021, Hounkpatin *et al.* 2022).

The PLS1 model demonstrated that LULC changes explained most of the variations in the water balance components in the basin. The regression coefficients show that the area of settlements/bare lands consistently is a key predictor of surface runoff, with a unit increase in settlements/bare lands enhancing runoff, likely due to restricted infiltration on impervious surfaces, and exposure of the bare soil surface to direct raindrops impact, thereby enhancing erosion and reducing infiltration (Togbévi *et al.* 2022). This suggests susceptibility to floods and a reduction in groundwater replenishment which has impacts on water availability for farming, domestic and industrial purposes. Conversely, a unit increase in forest areas was associated with a reduction in surface runoff, and an increase in subsurface flows, aquifer recharge and actual evapotranspiration. This is attributable to the dense canopy of forests which enables interception of rainfall, and the forest litter which inhibits runoff, thereby enhancing infiltration rates (Honda and Durigan 2016, Lokonon *et al.* 2019). A unit increase in agricultural lands increased surface runoff though lower compared to settlements/bare lands, and reduced subsurface flows and aquifer recharge, revealing the adverse impacts of extensive land degradation for agricultural expansion. Savanna areas experienced decreased surface runoff and increased subsurface flow, aquifer recharge and evapotranspiration, but at a lower potential than forests. This demonstrates the reduced ability of open tree canopy areas to effectively reduce runoff and enhance infiltration. These trends could aggravate water scarcity and reduction in ecosystem services in the basin (Togbévi *et al.* 2020). Furthermore, the Component 2 loadings of the PLS models indicate an increase in forest areas, agricultural lands and settlement areas, which corresponded with an increase in surface runoff and reduction in baseflow, aquifer recharge, and actual evapotranspiration. This suggests that the hydrological response of forest areas is more complex and potentially influenced by other factors such as land management practices (agro-forestry, selective logging, reforestation, impervious surfaces around trees), or fragmentation (continuous forests or small patches). This implies that reforestation efforts must ensure more continuous canopy coverage, while urban developments must consider more green areas around trees to enhance infiltration and reduce runoff.

4.3 Relationship between LULC and water balance components

The relationship between LULC changes and water balance components in this study predominantly reflects the wet-season conditions within the basin. The wet season contributed approximately 92% of the average annual rainfall (e.g. 1071.7 mm from 1155.7 mm average annual rainfall from 1998–2016), serving as a significant driver of the hydrological processes.

The high R^2 values obtained for surface runoff predictions across multiple periods suggest that the relationship between LULC change and runoff is robust and temporally consistent. This strong correlation reflects the immediate impact of reduced forest and savanna areas on surface runoff. However, the relatively lower R^2 values for baseflow, lateral flow, and total aquifer recharge across the three simulation periods (1998–2008, 2008–2016, and 1998–2016) indicate low generalizability, suggesting that these components are less sensitive to short-term LULC changes, are more dependent on temporal variability (more sensitive to other factors such as climate) and/or may have a non-linear relationship with LULC changes. Higher baseflow was estimated during the 16-year simulation period compared to the two 8-year periods. The Dahomeyan Basement, which underlies the study area, consists of metamorphic and crystalline rocks with inherently lower porosity and permeability, except where fractures are present (Faure and Volkoff 1998, Bossa 2012). However, there is no established link between geomorphic parameters and baseflow, although watershed geomorphology influences baseflow (Price 2011). Furthermore, the uncertainties in the SWAT model groundwater estimations could account for the inconsistencies in baseflow estimated for the different periods. This has necessitated the coupling of the SWAT model with groundwater models to adequately simulate baseflow (Bailey *et al.* 2020). Additionally, the minimal change in actual evapotranspiration, despite changes in LULC, can be attributed to the fact that expansion of tree crops such as cashew, orange, palm, and other plantations, which are quite abundant in parts of the basin, are able to maintain similar levels of evapotranspiration, compensating for the loss of natural forest and savanna areas (Ellison *et al.* 2012). Assessing the impacts of agricultural land expansion at the scale of specific crops may offer better insights into evapotranspiration trends.

The accurate prediction of surface runoff across the different periods indicates the consistency of its relationship with expanding urban and agricultural lands and diminishing natural vegetation. The increasing runoff volumes across the LULC maps hint at increasing flood potential in rapidly urbanizing areas, requiring urgent mitigation measures (Hounkpè *et al.* 2019, Nyatuame *et al.* 2020). At the same time, the reduction of baseflow and aquifer recharge has implications for long-term water availability for farming and domestic needs during the dry season (Togbévi and Sintondji 2021). Some of the challenges facing hydrological modelling include the complex nature of hydrological processes, limitations of the models and data variabilities and inaccuracies. Overall, the lack of long-term high-resolution data on precipitation, LULC and streamflow poses great challenge when modelling. The discrepancies between available "LULC data" and "hydrological modelling data" time frames in this study highlight these challenges. In data-scarce regions, like Africa particularly, inconsistencies in monitoring, human error or outdated measuring equipment introduces inaccuracies even where data exists (Giertz *et al.* 2006b, Bodjrènou *et al.* 2023).

5 Conclusions

This study assessed the relationship between LULC changes and changes in water balance across multiple periods in the Ouémé River basin, Benin. Surface runoff significantly increased by about 67% and an average annual amount of

31 mm whereas forest and savanna areas decreased by 4.9% and 24.1%, respectively. This relationship remained temporally consistent across the simulation periods (1998–2008, 2008–2016, and 1998–2016), emphasizing the link between LULC changes and surface runoff. Mainly, settlements/bare lands and forest areas were found as key predictors of surface runoff, with expansion in settlements/bare lands increasing surface runoff while forest cover reduced it. Savanna areas reduced runoff but at a lower extent than forests, while agricultural lands also increased runoff at a lower extent than settlements/bare lands.

Baseflow, lateral flow, total aquifer recharge and actual evapotranspiration showed a declining trend as forest and savanna areas decreased and agricultural and settlements/bare land increased. The strong correlations between water balance components and LULC changes indicate a substantial link between LULC and hydrological responses, even though they do not fully explain the physical mechanisms driving these changes. The high R^2 values (>0.75) from the cross-period prediction of surface runoff suggest that it is a reliable indicator of changes in hydrological processes due to land management practices. On the other hand, baseflow, lateral flow, aquifer recharge and actual evapotranspiration showed low predictability across periods. Actual evapotranspiration showed minute changes across LULC maps, suggesting compensating capabilities of tree crops in offsetting the loss of natural forests and savanna areas in the basin.

Overall, this study highlights the significant role of LULC changes in shaping hydrological processes in the Ouémé River basin while acknowledging the influence of other factors such as catchment characteristics, subsurface processes and climate variability, which require further investigation. In particular, watershed attributes such as area, channel properties, topography, soil type, etc., may influence hydrological processes. However, these attributes do not change simply over time, especially considering our study period. Therefore, our study focused on the impact of LULC on water balance. The findings underscore the need for sustainable land management practices, including reforestation, permanent cover crops, minimum tillage, agroforestry, and green urban spaces to mitigate flooding risks. Future studies should explore the influence of LULC on water balance at the sub-basin scale and investigate seasonal variations in the LULC–water balance relationship.

Acknowledgements

he authors thank the BMBF ("Bundesministerium für Bildung und Forschung") for funding the PhD research of Ernestina Annan under the West African Science Service Center on Climate Change and Adapted Land Use (WASCAL) programme. Moreover, we thank the BMBF for the funding of the FURIFLOOD research project ("Current and future risks of urban and rural flooding in West Africa," Grant No.: 01LG2086B). We thank our partners involved in the FURIFLOOD project for their support. This work was further supported by the European Union's Horizon Europe research and innovation programme as part of the UAWOS project ("Unmanned Airborne Water Observing System," Grant Agreement No.: 101081783).

Disclosure statement

No potential conflict of interest was reported by the author(s).

ORCID

Ernestina Annan http://orcid.org/0000-0002-5466-6460
William Amponsah http://orcid.org/0000-0002-1010-1206
Kwaku Amaning Adjei http://orcid.org/0000-0003-3220-6735
Markus Disse http://orcid.org/0000-0003-4620-575X
Wilson Agyei Agyare http://orcid.org/0000-0002-4028-7961

References

Abbaspour, K.C., 2015. *SWAT-CUP SWAT Calibration and Uncertainty Programs (CUP) – a user manual*. Eawag, Duebendorf: Swiss Federal Institute of Aquatic Science and Technology.

Abdi, H., 2010. Partial least squares regression and projection on latent structure regression (PLS Regression). *Wiley Interdisciplinary Reviews: Computational Statistics*, 2 (1), 97–106. doi:10.1002/wics.51

Abdulkadir, T.S., *et al.*, 2022. Prediction of water yield and balance in Upper Oueme River Catchment in Benin Republic. *Bayero Journal of Engineering and Technology (BJET)*, 17 (1), 41–52.

Adjei, F.O., *et al.*, 2023. Evaluation of potential evapotranspiration assessment methods for hydrological modelling with SWAT in the Densu river basin in Ghana. *International Journal of Environmental Science and Technology*, 20 (1), 921–930. doi:10.1007/s13762-022-03945-y

Aladejana, O., Salami, A., and Adetoro, O., 2018. Hydrological responses to land degradation in the Northwest Benin Owena River Basin, Nigeria. *Journal of Environmental Management*, 225, 300–312. doi:10.1016/j.jenvman.2018.07.095

Annan, E., *et al.*, 2024. Spatio-temporal land use and land cover change assessment: insights from the Ouémé River Basin. *Scientific African*, 25, 1–11. doi:10.1016/j.sciaf.2024.e02262

Arnold, J.G., *et al.*, 1998. Large area hydrologic modeling and assessment part I: model development. *Journal of the American Water Resources Association*, 34 (1), 73–89. doi:10.1111/j.1752-1688.1998.tb05961.x

Arnold, J.G., *et al.*, 2013. *SWAT 2012 input/output documentation* (TR-439). Statewide, TX: Texas Water Resources Institute.

Bailey, R.T., *et al.*, 2020. Enhancing SWAT+ simulation of groundwater flow and groundwater-surface water interactions using MODFLOW routines. *Environmental Modelling and Software*, 126, 1–14. doi:10.1016/j.envsoft.2020.104660

Bodjrènou, R., Sintondji, L.O., and Comandan, F., 2023. Hydrological modeling with physics-based models in the Ouémé basin: issues and perspectives for simulation optimization. *Journal of Hydrology: Regional Studies*, 48, 1–14.

Bossa, A.Y., Diekkrüger, B., and Agbossou, E.K., 2014. Scenario-based impacts of land use and climate change on land and water degradation from the meso to regional scale. *Water (Switzerland)*, 6 (10), 3152–3181.

Bossa, Y.A., 2012. *Multi-scale modeling of sediment and nutrient flow dynamics in the Ouémé catchment (Benin) – towards an assessment of global change effects on soil degradation and water quality*. Thesis (PhD). Universität Bonn.

Dossou, J.F., *et al.*, 2021. Impact of agriculture on the Oueme Basin in Benin. *Water, Air, and Soil Pollution*, 232 (12), 1–21. doi:10.1007/s11270-021-05397-5

Ellison, D., Futter, M.N., and Bishop, K., 2012. On the forest cover-water yield debate: from demand- to supply-side thinking. *Global Change Biology*, 18 (3), 806–820. doi:10.1111/j.1365-2486.2011.02589.x

Faure, P. and Volkoff, B., 1998. Some factors affecting regional differentiation of the soils in the Republic of Benin (West Africa). *Catena*, 32 (3–4), 281–306. doi:10.1016/S0341-8162(98)00038-1

Fisher, J.R.B., *et al.*, 2018. Impact of satellite imagery spatial resolution on land use classification accuracy and modeled water quality. *Remote Sensing in Ecology and Conservation*, 4 (2), 137–149. doi:10.1002/rse2.61

Forbes, T.R., 1973. This review of the literature on ferrallitic and ferruginous tropical. *In*: Agronomy mimeo. Ithaca, New York: Cornell University, 73–20.

Geladi, P. and Kowalski, B., 1986. Partial least-sqaures regression: a tutorial. *Analytica Chimica Acta*, 185, 1–17. doi:10.1016/0003-2670(86)80028-9

Giertz, S., *et al*., 2006a. An interdisciplinary scenario analysis to assess the water availability and water consumption in the Upper Ouémé catchment in Benin. *Advance in Geosciences*, 9. Available from: www.adv-geosci.net/9/3/2006/

Giertz, S., Diekkrüger, B., and Steup, G., 2006b. Physically-based modelling of hydrological processes in a tropical headwater catchment (West Africa)- process representation and multi-criteria validation. *In*: *Hydrology and earth system sciences*, Vol. 10, 829–847. doi:10.5194/hess-10-829-2006

Hargreaves, G.H. and Samani, Z.A., 1985. Reference crop evapotranspiration from temperature. *Applied Engineering in Agriculture*, 1 (2), 96–99. doi:10.13031/2013.26773

Hiepe, C., 2008. *Soil degradation by water erosion in a sub-humid West-African catchment: a modelling approach considering land use and climate change in Benin*. Thesis (PhD). Universität Bonn.

Honda, E.A. and Durigan, G., 2016. Woody encroachment and its consequences on hydrological processes in the Savannah. *Philosophical Transactions of the Royal Society B*, 371 (1703), 1–9. doi:10.1098/rstb.2015.0313

Hounkpatin, K.O.L., *et al*., 2022. Assessment of the soil fertility status in Benin (West Africa) – digital soil mapping using machine learning. *Geoderma Regional*, 28, 1–14. doi:10.1016/j.geodrs.2021.e00444

Hounkpè, 2016. *Assessing the climate and land use changes impact on flood hazard in Ouémé River Basin, Benin (West Africa)*. Thesis (PhD). University of Abomey Calavi.

Hounkpè, J., *et al*., 2019. Land use change increases flood hazard: a multi-modelling approach to assess change in flood characteristics driven by socio-economic land use change scenarios. *Natural Hazards*, 98 (3), 1021–1050. doi:10.1007/s11069-018-3557-8

Hounkpè, J. and Diekkrüger, B., 2018. Challenges in calibrating hydrological models to simultaneously evaluate water resources and flood hazard: a case study of Zou basin, Benin. *Episodes*, 41 (2), 105–114. doi:10.18814/epiiugs/2018/018010

Houssou, A.M., *et al*., 2017. Spatial and seasonal characterization of water quality in the Ouémé River basin (Republic of Benin, West Africa). *Egyptian Journal of Chemistry*, 60 (6), 1077–1090. doi:10.21608/ejchem.2017.1463.1095

Kilinzo, F., *et al*., 2011. Selecting a Potential Evapotranspitration (PET) method in the absence of essential climatic input data. *In*: *SWAT International Conference-TOLEDO*. Spain: Texas A&M University.

Lokonon, B.E., *et al*., 2019. Knowledge, valuation and prioritization of 46 woody species for conservation in agroforestry systems along Ouémé catchment in Benin (West Africa). *Environment, Development and Sustainability*, 21 (5), 2377–2399. doi:10.1007/s10668-018-0142-y

Mbaye, M.L., *et al*., 2015. Assessment of climate change impact on water resources in the upper Senegal Basin (West Africa). *American Journal of Climate Change*, 4 (1), 77–93. doi:10.4236/ajcc.2015.41008

Merk, F., *et al*., 2024. The significance of the leaf-area-index on the evapotranspiration estimation in SWAT-T for characteristic land cover types of Western Africa. *Hydrology and Earth System Sciences*, 28 (24), 5511–5539. doi:10.5194/hess-28-5511-2024

Moriasi, D.N., *et al*., 2007. Model evaluation guidelines for systematic quantification of accuracy in watershed simulations. *Transactions of the ASABE*, 50 (3), 885–900. doi:10.13031/2013.23153

Mosavi, A., *et al*., 2020. Susceptibility mapping of soil water erosion using machine learning models. *Water (Switzerland)*, 12 (7), 1–17.

Neitsch, S.L., *et al*., 2002. *Soil and water assessment tool user's manual version 2000*. Temple, Texas: Grassland, Soil and Water Research Laboratory, Agricultural Research Service.

Nyatuame, M., Amekudzi, L.K., and Agodzo, S.K., 2020. Assessing the land use/land cover and climate change impact on water balance on tordzie watershed. *Remote Sensing Applications: Society and Environment*, 20, 1–10.

Odusanya, A.E., *et al*., 2021. Evaluating the performance of streamflow simulated by an eco-hydrological model calibrated and validated with global land surface actual evapotranspiration from remote sensing at a catchment scale in West Africa. *Journal of Hydrology: Regional Studies*, 37, 1–22.

Olofintoye, O.O., *et al*., 2022. A study on the applicability of a SWAT model in predicting the water yield and water balance of the Upper Ouémé catchment in the Republic of Benin. *Slovak Journal of Civil Engineering*, 30 (1), 57–66. doi:10.2478/sjce-2022-0007

Osseni, A.A., *et al*., 2022. Spatial dynamics and predictive analysis of vegetation cover in the Ouémé river Delta in Benin (West Africa). *Remote Sensing*, 14 (23), 1–19. doi:10.3390/rs14236165

Pirouz, D.M., 2006. *An overview of partial least squares*. Irvine: The Paul Merage School of Business, University of California. Available from: http://www.merage.uci.edu/~dpirouz04/

Price, K., 2011. Effects of watershed topography, soils, land use, and climate on baseflow hydrology in humid regions: a review. *Progress in Physical Geography*, 35 (4), 465–492. doi:10.1177/0309133311402714

Rauch, M., *et al*., 2024. Geostatistical simulation of daily rainfall fields - performance assessment for extremes in West Africa. *Journal of Hydrometeorology*, 25 (10), 1425–1442. doi:10.1175/JHM-D-23-0123.1

Ritchie, J.T., 1972. Model for predicting evaporation from a row crop with incomplete cover. *Water Resources Research*, 8 (5), 1204–1213. doi:10.1029/WR008i005p01204

Saddique, N., Mahmood, T., and Bernhofer, C., 2020. Quantifying the impacts of land use/land cover change on the water balance in the afforested River Basin, Pakistan. *Environmental Earth Sciences*, 79 (19), 1–13. doi:10.1007/s12665-020-09206-w

Sintondji, L.O., *et al*., 2014. Modelling the water balance of Ouémé catchment. *International Journal of Agricultural Science*, 4 (1), 74–88.

Togbévi, Q., *et al*., 2020. A multi-model approach for analysing water balance and water related ecosystem services in the Ouriyori catchment (Benin). *Hydrological Science Journal*, 65 (14), 2453–2465. doi:10.1080/02626667.2020.1811286

Togbévi, Q., *et al*., 2022. Assessing the effects of anthropogenic land use on soil infitration rates in a tropical West African Watershed (Ouriyori, Benin). *Applied and Environmental Soil Science*, 2022, 1–11. doi:10.1155/2022/8565571

Togbévi, Q.F. and Sintondji, L.O., 2021. Hydrological response to land use and land cover changes in a tropical West African catchment (Couffo, Benin). *AIMS Geosciences*, 7 (3), 338–354. doi:10.3934/geosci.2021021

White, J.W., *et al*., 2014. Ecologists should not use statistical significance tests to interpret simulation model results. *Oikos*, 123 (4), 385–388. doi:10.1111/j.1600-0706.2013.01073.x

Appendix

1. *SWAT model performance metric equations*

$$NS = 1 - \frac{\sum_i (Q_{obs} - Q_{sim})_i^2}{\sum_i \left(Q_{obs,i} - \overline{Q}_{obs}\right)^2} \tag{A1}$$

$$PBIAS = 100\left(\frac{\sum_{I=1}^{n} (Q_{obs} - Q_{sim})_i}{\sum_{i=1}^{n} Q_{obs,i}}\right) \tag{A2}$$

$$KGE = 1 - \sqrt{(r-1)^2 + (\alpha - 1)^2 + (\beta - 1)^2} \tag{A3}$$

$$RSR = \frac{\sqrt{\sum_{i=1}^{n} (Q_{obs} - Q_{sim})_i^2}}{\sqrt{\sum_{i=1}^{n} \left(Q_{obs,i} - \overline{Q}_{obs}\right)^2}} \tag{A4}$$

$$R^2 = \frac{\left[\sum_i (Q_{obs,i} - \overline{Q}_{obs})(Q_{sim,i} - \overline{Q}_{sim})\right]^2}{\sum_i \left(Q_{obs,i} - \overline{Q}_{obs}\right)^2 (Q_{sim,i} - \overline{Q}_{sim})^2} \tag{A5}$$

where:

Q_{obs} and Q_{sim} are observed and simulated discharge (m^3/s),

$\overline{Q}_{obs}$ and $\overline{Q}_{sim}$ are mean observed and simulated discharge, respectively, and (σ and β are mean and standard deviation, respectively).

2. *Partial least squares (PLS) regression*

PLS is a linear regression model which explains the covariance between a set of dependent (predictor) and independent (response) variables by simultaneously decomposing them into latent variables using Equations (A6) and (A7), when the predictors are strongly correlated. We refer readers to Abdi (2010) and Geladi and Kowalski (1986) for further reading.

$$X = TP^T + E \tag{A6}$$

$$Y = UQ^T + F \tag{A7}$$

where:

X is the matrix of the predictor variables

Y is the matrix of the response variables

T is the matrix of latent scores for X

P is the matrix of loadings for X

U is the matrix of latent scores for Y

Q is the matrix of loadings for Y

E and F are error terms (residuals) of X and Y